



NETWORK NEURO SCIENCE

an open access  journal



Citation: Sheheittli, H., & Jirsa, V. K. (2020). A mathematical model of ephaptic interactions in neuronal fiber pathways: Could there be more than transmission along the tracts? *Network Neuroscience*, 4(3), 595–610. https://doi.org/10.1162/netn_a_00134

DOI:
https://doi.org/10.1162/netn_a_00134

Supporting Information:
https://doi.org/10.1162/netn_a_00134

Received: 8 September 2019
Accepted: 26 February 2020

Corresponding Author:
Hiba Sheheittli
hs497@cornell.edu

Handling Editor:
Mason Porter

Copyright: © 2020
Massachusetts Institute of Technology
Published under a Creative Commons
Attribution 4.0 International
(CC BY 4.0) license



RESEARCH

A mathematical model of ephaptic interactions in neuronal fiber pathways: Could there be more than transmission along the tracts?

Hiba Sheheittli¹ and Viktor K. Jirsa¹

¹Aix-Marseille University, Inserm, INS UMR_S 1106, Marseille, France

Keywords: Ephaptic interaction modeling, Axonal cable theory, Fiber pathways, Neuronal communication, White matter, Spatiotemporal patterns

ABSTRACT

While numerous studies of ephaptic interactions have focused on either axons of peripheral nerves or on cortical structures, no attention has been given to the possibility of ephaptic interactions in white matter tracts. Inspired by the highly organized, tightly packed geometry of axons in fiber pathways, we aim to investigate the potential effects of ephaptic interactions along these structures that are resilient to experimental probing. We use axonal cable theory to derive a minimal model of a sheet of N ephaptically coupled axons. Numerical solutions of the proposed model are explored as ephaptic coupling is varied. We demonstrate that ephaptic interactions can lead to local phase locking between adjacent traveling impulses and that, as coupling is increased, traveling impulses trigger new impulses along adjacent axons, resulting in finite size traveling fronts. For strong enough coupling, impulses propagate laterally and backwards, resulting in complex spatiotemporal patterns. While common large-scale brain network models often model fiber pathways as simple relays of signals between different brain regions, our work calls for a closer reexamination of the validity of such a view. The results suggest that in the presence of significant ephaptic interactions, the brain fiber tracts can act as a dynamic active medium.

AUTHOR SUMMARY

Starting from the FitzHugh-Nagumo cable model, we derive a system of nonlinear coupled partial differential equations (PDEs) to model a sheet of N ephaptically coupled axons. We also present a continuous limit approximation transforming the model into a two-dimensional field equation. We numerically solve the equations exploring the dynamics as coupling strength is varied. We observe phase locking of adjacent impulses and coordination of subthreshold dynamics. Strong enough coupling generates complex spatiotemporal patterns as new impulses form traveling fronts propagating laterally and backwards. The transition between different dynamic regimes happens abruptly at critical values of parameter. The results put into question the validity of assuming the role of fiber pathways to be that of mere interneuronal transmission and call for further investigation of the matter.

INTRODUCTION

It has long been thought that signals exchanged between different brain regions are faithfully transmitted along the white matter tracts through axons that can be modeled as passive electric cables (Hodgkin & Huxley, 1952). This has led many large-scale network models to assume

Ephaptic interaction:
A form of indirect communication between cells through the exchange of ions via the shared extracellular space.

that signals communicated between different brain regions are relayed along the axons of fiber pathways with a finite speed without any interaction occurring between the traveling signals along the way (Bassett, Zurn, & Gold, 2018; Breakspear, 2017; Sanz-Leon, Knock, Spiegler, & Jirsa, 2015). The aim of this work is to motivate a reexamination of this latter highly consequential assumption. In 1940, Katz and Schmitt investigated the nonsynaptic electrical interaction between adjacent nerve fibers (Katz & Schmitt, 1940). In their work, two large parallel non-myelinated axons were isolated from the crab limb nerve. They succeeded in demonstrating that (a) the passage of an action potential (impulse) in one fiber causes subthreshold excitability changes in the adjacent fiber and (b) when impulses are set up simultaneously along both fibers, a mutual interaction occurs that can lead to speeding up or slowing down of the impulses and also possibly to synchronization between the two impulses, depending on the initial phase relationship. The effect was observed to be amplified when the resistance of the extracellular space surrounding the axons was increased. In the next year, a similar study was presented by Arvanitaki (1942) on giant axons of *Sepia officinalis* (common cuttlefish). In that study, Arvanitaki coined the term “ephapse” to denote “the locus of contact or close vicinity of two active functional surfaces” (p. 90). The term is derived from the Greek term signifying the act of touching, as opposed to “synapse” which is derived from the Greek term signifying the act of joining or linking. Since then, the term ephaptic interaction has been used to refer to communication between neuronal cells via electrical conduction through the surrounding extracellular space, as opposed to communication mediated by chemical synapses or gap-junctions. In 1980, ephaptic transmission was observed between spontaneously active single nerve fibers in the spinal nerve roots of dystrophic mice (Rasminsky, 1980). Shortly after, ephaptic interactions were observed to contribute to neuronal synchrony in rat hippocampal slices (Taylor & Dudek, 1982). Then in 1984, experiments suggested a role for ephaptic transmission in hemifacial spasm pathophysiology by causing “cross-talk” between facial nerve fibers (Nielsen, 1984). More recently, hallmarks of ephaptic interaction were observed in rat cortical pyramidal neurons in slices, and supported the idea that this interaction facilitates the coordination and possibly the synchrony of neighboring neurons in the gray matter (Anastassiou, Perin, Markram, & Koch, 2011). In addition, there have been numerous other experimental and modeling investigations of ephaptic interaction (Anastassiou & Koch, 2015; Barr & Plonsey, 1992; Bell, 1981; Bokil, Laaris, Blinder, Ennis, & Keller, 2001; Goldwyn & Rinzel, 2016; Grindrod & Sleeman, 1984; Holt & Koch, 1999; Ramón & Moore, 1978; Stacey, Hilbert, & Quail, 2015). However, it can be seen that all these previous studies focused on one of two contexts: (a) cortical areas, particularly interactions between neighboring neurons through the resulting local field potential (Anastassiou & Koch, 2015; Anastassiou et al., 2011; Blot & Barbour, 2014; Fröhlich & McCormick, 2010; Goldwyn & Rinzel, 2016; Holt & Koch, 1999; Taylor & Dudek, 1982) or (b) peripheral nerves, particularly interactions between myelinated axons in a nerve bundle and inquiries into effects of demyelination (Binczak, Eilbeck, & Scott, 2001; J. W. Clark & Plonsey, 1970; Marrazzi & Lorente, 1944; Nielsen, 1984; Ramón & Moore, 1978; Rasminsky, 1980; Reutskiy, Rossoni, & Tirozzi, 2003). To our knowledge, there has been no discussion on ephaptic interaction between axons of the white matter tracts. While the predominant myelination in white matter axons might be presumed to be preventing ephaptic interference, studies of myelinated axons in nerves suggest otherwise (Binczak et al., 2001; Marrazzi & Lorente, 1944; Rosenblueth, 1941). Moreover, some fiber pathways can have a considerably high proportion of unmyelinated axons, such as 30% (in regions of the corpus callosum of the adult rhesus monkey; Lamantia & Rakic, 1990) and 45% (in the splenium of the corpus callosum of the adult rabbit; Waxman & Swadlow, 1977). It is known that fiber pathways in the brain are constituted of densely packed long axons running in parallel. In Wedeen et al. (2012), diffusion magnetic resonance imaging results were presented to illustrate that “cerebral path

crossings formed well-defined 2D sheets” (p. 1631) and that “this sheet structure was found throughout cerebral white matter and in all species, orientations, and curvatures. Moreover, no brain pathways were observed without sheet structure” (Wedeen et al., 2012, p. 1632). In addition, electron micrograph images show that neighboring axons in fiber pathways are often separated by distances as small as 20 nm (Waxman & Swadlow, 1977), which would suggest a relatively high extracellular space resistance. These latter geometric characteristics set favorable conditions for ephaptic exchanges to be at play in white matter fiber pathways. Ideally, direct experimental examination of the activity of axons in the white matter would serve to accurately quantify ephaptic interactions there. However, probing into the inner workings of the white matter remains a challenging endeavor, mainly because of technical limitations on the temporal and spatial resolution of current noninvasive imaging techniques (He, Yang, Wilke, & Yuan, 2011). Inspired by these facts, we wish to investigate the matter by putting forward a simple but realistic mathematical model of excitable axons arranged in a sheetlike geometry and coupled through a resistive extracellular space.

In the Materials and Methods, we start from local circuit theory and the cable model of an axon to derive a model for a sheet of N ephaptically coupled axons. We then make a continuous limit approximation to transform the resulting model of N coupled 1D partial differential equations (PDEs) into a 2D PDE that can be seen as a field equation governing the dynamics of a sheet of coupled axons. In the Results section, we numerically solve the equations and explore the different possible dynamical regimes along with examining the equivalence of the two proposed models. In the Discussion section, we discuss the potential ramifications of the results along with future work directions that this work motivates.

MATERIALS AND METHODS

The Mathematical Model

Our goal here is to put forward a minimal model that possesses the key elements that allow the study of the effects of ephaptic interactions on action potential transmission along fiber pathways. Given the densely packed parallel geometric arrangement of axons in the white matter, we assume that currents generated during action potential propagation are mainly axial in direction, both inside the axons and in the surrounding extracellular space (J. Clark & Plonsey, 1968; Plonsey, 1977). Then the axons can be represented by what is known as the cable equation, while the extracellular space between axons can be represented by an effective longitudinal resistance per unit length (Rall, 1962; Scott, 2002). Such a model for two ephaptically coupled axons is derived in Bell (1981). Figure 1 depicts the equivalent circuit model used to derive the cable equations for two ephaptically coupled axons. The following notation is used here:

- i^a : axial (axoplasmic) current inside the axon per unit length
- i^e : axial current in the extracellular space surrounding the axons per unit length
- i^m : axonal transmembrane current per unit area
- r_a : axoplasmic resistance per unit length
- r_e : extracellular space resistance per unit length
- c : axonal membrane capacitance per unit length
- j_{ion} : active ionic current flowing across the axonal membrane per unit length
- g : membrane conductance per unit length
- z : distance along the axon
- v^m : transmembrane potential of an axon

Cable equation:

A partial differential equation describing the evolution of cell membrane voltage and currents as functions of distance and time.

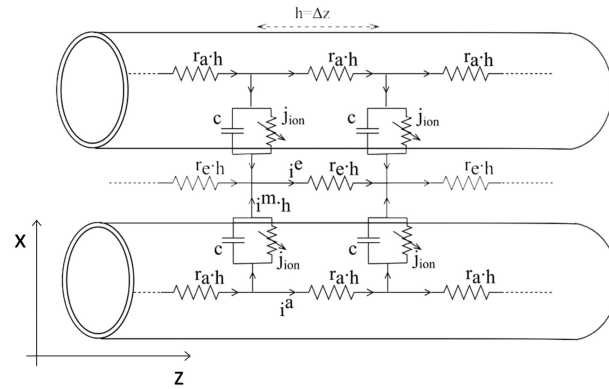


Figure 1. Schematic of the equivalent circuit model for two ephaptically coupled axons.

- v^a : axoplasmic potential inside an axon
- v^e : electric potential in the extracellular space
- I : external applied current per unit length
- a, b : parameters of the FitzHugh-Nagumo model

Here, all currents and potential variables are varying functions of time and axial location z .

Kirchoff's law:
The law of conservation of electric charge.

In the limit of $\Delta z \rightarrow 0$, Kirchoff's current law gives the following relationships between the transmembrane, axial, and extracellular currents; subscripts 1 and 2 each refer to one of the two identical axons:

$$i_1^m = -\frac{\partial i_1^a}{\partial z}, \quad i_2^m = -\frac{\partial i_2^a}{\partial z}; \quad (1)$$

$$\frac{\partial i^e}{\partial z} = i_1^m + i_2^m. \quad (2)$$

Ohm's law:
The law of proportionality between the electric current and voltage across a conductor.

In addition, Ohm's law relates the currents to the electric potentials as follows:

$$\frac{\partial v_1^a}{\partial z} = -r_a i_1^a, \quad \frac{\partial v_2^a}{\partial z} = -r_a i_2^a, \quad \frac{\partial v^e}{\partial z} = -r_e i^e. \quad (3)$$

Furthermore, the transmembrane current for each axon can be expressed as

$$i^m = c \frac{\partial v^m}{\partial t} + j_{ion} - I, \quad \text{where } v^m = v^a - v^e. \quad (4)$$

The term j_{ion} represents the active transmembrane currents due to ion channel activity that is nonlinearly dependent on the transmembrane voltage. Detailed mathematical representation of the dependence of j_{ion} on v^m was described in the seminal work by Hodgkin and Huxley (1952), which utilized three variables to represent the kinetics of ion channel activation. In 1961, FitzHugh proposed a simplification of that model that utilizes only one recovery variable (FitzHugh, 1961):

$$j_{ion} = gf(v^m, w), \quad \text{where } f(v, w) = -\left(v - \frac{v^3}{3} - w\right) \quad (5)$$

$$\text{with } \frac{\partial w}{\partial t} = \varepsilon(v + a - bw).$$

Here, w is a slow recovery variable. To arrive at the cable equation model, we need to combine all the above relationships to eliminate the current variables. We start by differentiating the

expression for v^m with respect to z and substituting Equation 3 in it:

$$\frac{\partial v_1^m}{\partial z} = -r_a i_1^a + r_e i^e, \quad \frac{\partial v_2^m}{\partial z} = -r_a i_2^a + r_e i^e.$$

Differentiating again and substituting Equation 1, we obtain the following:

$$\begin{aligned} \frac{\partial^2 v_1^m}{\partial z^2} &= (r_a + r_e) i_1^m + r_e i_2^m, \\ \frac{\partial^2 v_2^m}{\partial z^2} &= (r_a + r_e) i_2^m + r_e i_1^m. \end{aligned} \tag{6}$$

Solving the above system of two equations for an expression for i_1^m and i_2^m , then combining the result with Equation 4, we arrive at the cable equations for two ephaptically coupled axons:

$$\begin{aligned} \gamma \frac{\partial^2 v_1^m}{\partial z^2} - \alpha \frac{\partial^2 v_2^m}{\partial z^2} &= c \frac{\partial v_1^m}{\partial t} + j_{ion,1} - I_1, \\ \gamma \frac{\partial^2 v_2^m}{\partial z^2} - \alpha \frac{\partial^2 v_1^m}{\partial z^2} &= c \frac{\partial v_2^m}{\partial t} + j_{ion,2} - I_2, \end{aligned} \tag{7}$$

where $\gamma = \left(\frac{r_a + r_e}{2r_a r_e + r_a^2} \right)$, $\alpha = \left(\frac{r_e}{2r_a r_e + r_a^2} \right)$.

We can see that for zero extracellular resistance, the two cable equations are uncoupled such that any current exiting one axon will immediately dissipate in the extracellular space and no exchange between the axons can occur. The resulting single FitzHugh-Nagumo cable was first put forward by Nagumo in Nagumo, Arimoto, and Yoshizawa (1962). It can be seen that the cable equation is the classical 1D diffusion equation with an added term, j_{ion} . The presence of the nonlinear active currents renders the cable excitable, such that, if the membrane potential is perturbed from its resting value, it will return to that value unless the perturbation is strong enough to elicit the large action potential response that will then be propagated along the axon, away from the location of perturbation, with the signal's shape preserved.

We wish to extend the model to a sheet of ephaptically coupled axons, that is, an N number of axons coupled through the extracellular space. Figure 2 shows a schematic of a cross-sectional view of such an arrangement where we represent the cross sections of axonal cables as nodes on a line, interspaced with nodes representing extracellular space.

A model of such a configuration of N number of coupled axons was presented in Grindrod and Sleeman (1984). The main assumption made in this latter work is that each axon is only coupled to the two axons that are positioned directly next to it. While this later assumption is common in network models, the authors offered no physiological justification for it in the context of ephaptically coupled axons. Instead, we will start from the more physical assumption that transmembrane currents are radially uniform, such that we can reasonably consider i^m for each cable to be equally partitioned into two parts feeding into the extracellular space (represented as nodes) adjacent to it. Consequently, while the previously presented model

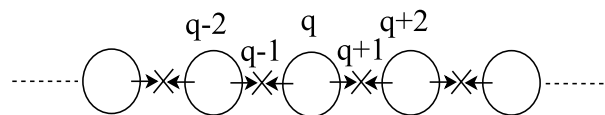


Figure 2. Schematic of a cross-sectional view of the sheet of N axons model.

restricts ephaptic interactions to nearest neighbor axons (Grindrod & Sleeman, 1984), our model allows each axon to interact with all other axons through the shared extracellular space with the coupling strength decaying with distance between interacting axons. To arrive at that, we take the potential in the extracellular space for an axon positioned at a node q to be the average of the potential at its adjacent extracellular nodes such that

$$v_q^m = v_q^a - \frac{1}{2} (v_{q-1}^e + v_{q+1}^e). \quad (8)$$

Note that the index q refers to the node number on the line, so for N axons, q takes values between 1 and $2N + 1$, such that v_q^a is defined on nodes $q = 2, 4, \dots, N$ and v_q^e on nodes $q = 1, 3, \dots, N + 1$. Differentiating Equation 8 with respect to z , and making use of Ohm's law, we obtain

$$\frac{\partial v_q^m}{\partial z} = -r_a i_q^a + \frac{1}{2} r_e (i_{q-1}^e + i_{q+1}^e). \quad (9)$$

From Kirchoff's first law of current, we have the following:

$$\begin{aligned} \frac{\partial i_q^a}{\partial z} &= -i_q^m, \\ \frac{\partial i_{q-1}^e}{\partial z} &= \frac{1}{2} (i_{q-2}^m + i_q^m), \\ \frac{\partial i_{q+1}^e}{\partial z} &= \frac{1}{2} (i_{q+2}^m + i_q^m). \end{aligned}$$

These latter equations are a generalization of Equations 1 and 2. Differentiating Equation 9 again and plugging in the above current relationships, we arrive at

$$\frac{\partial^2 v_q^m}{\partial z^2} = \left(r_a + \frac{1}{2} r_e \right) i_q^m + \frac{1}{4} r_e (i_{q-2}^m + i_{q+2}^m). \quad (10)$$

For the cables that are at the two ends of the line, the corresponding relationship would be the following:

$$\begin{aligned} \frac{\partial^2 v_2^m}{\partial z^2} &= \left(r_a + \frac{1}{2} r_e \right) i_2^m + \frac{1}{4} r_e (i_4^m), \\ \frac{\partial^2 v_N^m}{\partial z^2} &= \left(r_a + \frac{1}{2} r_e \right) i_N^m + \frac{1}{4} r_e (i_{N-2}^m). \end{aligned}$$

We have obtained a system of N equations relating i^m and v^m of all the axons. This is the equivalent of Equation 6 for the two-axon system. The linear system of N equations can be solved, such that we can express each i^m explicitly in terms of v^m of all the axons. The solution takes the form

$$i_p^m = \frac{4}{r_e} \sum_{s=1}^N \alpha_{ps} \frac{\partial^2 v_s^m}{\partial z^2}; \quad (11)$$

$p = 1, 2, \dots, N$ referring to the N axons. The α 's represent coupling strength between each pair of axons and are obtained as the elements of the inverse matrix $A^{-1} = [\alpha_{ij}]$, where A is the tridiagonal matrix:

$$A = \begin{bmatrix} D & 1 & & & & & \\ 1 & D & 1 & & & & \\ & & 1 & D & 1 & & \\ & & & \ddots & \ddots & \ddots & \\ & & & & \ddots & \ddots & \ddots \\ & & & & & 1 & D & 1 \\ & & & & & & 1 & D & 1 \\ & & & & & & & 1 & D \end{bmatrix} \quad \text{with } D = 4 \left(R + \frac{1}{2} \right) \text{ and } R = \frac{r_a}{r_e}.$$

Explicit algebraic expressions for the elements of the inverse of such a tridiagonal matrix are presented in Usmani (1987) and indicate that the ephaptic effect increases as the ratio R decreases and that α for two axons on the line decreases as the distance between them increases. However, for the numerical solutions presented in the sections to follow, we found it simpler to numerically compute the inverse of A instead of the individual α 's.

Combining Equations 11, 5, and 4, we obtain the model for a sheet of N ephaptically coupled FitzHugh-Nagumo cables:

$$\frac{4}{r_e} \sum_{s=1}^N \alpha_{ps} \frac{\partial^2 v_s^m}{\partial z^2} = c \frac{\partial v_p^m}{\partial t} + g f(v_p^m, w_p) - I_p, \tag{12}$$

$$\frac{\partial w_p}{\partial t} = \varepsilon (v_p^m + a - b w_p).$$

We nondimensionalize the space and time variables as follows:

$$\tilde{z} = \left(\sqrt{g(r_a + r_e)} \right) z, \quad \tilde{t} = \frac{g}{c} t.$$

The system becomes

$$4(R + 1) \sum_{s=1}^N \alpha_{ps} \frac{\partial^2 v_s^m}{\partial \tilde{z}^2} = \frac{\partial v_p^m}{\partial \tilde{t}} + f(v_p^m) - \hat{I}_p,$$

$$\frac{\partial w_p}{\partial \tilde{t}} = \hat{\varepsilon} (v_p^m + a - b w_p),$$

where $\hat{I}_p = \frac{I}{g}$, $\hat{\varepsilon} = \varepsilon \frac{c}{g}$.

From now on, we drop the superscript of the transmembrane voltage along with the tilde and hat. The final equations take the following form:

$$4(R + 1) \sum_{s=1}^N \alpha_{ps} \frac{\partial^2 v_s}{\partial z^2} = \frac{\partial v_p}{\partial t} + f(v_p, w_p) - I_p, \tag{13}$$

$$\frac{\partial w_p}{\partial t} = \varepsilon (v_p + a - b w_p).$$

For the results that will follow, we choose the following values for the FitzHugh-Nagumo recovery variable: $a = 0.7$, $b = 0.5$, and $\varepsilon = 0.1$. Then, we are left with one free parameter R that reflects the strength of the ephaptic interaction. The goal is to investigate the dynamics of the system as this parameter is varied. We note here that the resulting emergent network

behavior is robust against variations of the FitzHugh-Nagumo parameters within a reasonable range that preserves the relevant dynamic features of the neuron model (planar, class 1 in terms of excitability, existence of refractory period, and slow manifold). Multiple parameters were tried, and only one example is presented here for brevity.

Estimation of the Coupling Strength Parameter

To estimate the physically plausible range of values for parameter R , we start from the definition

$$R = \frac{r_a}{r_e} = \frac{1}{\rho} \frac{A_e}{A_a},$$

where A_e and A_a are the cross-sectional areas of the extracellular space and the axon, respectively. ρ is the ratio of extracellular to intracellular resistivity, and is typically assumed to be in the range of 1 to 4 (Goldwyn & Rinzel, 2016). Given that axons of the fiber pathways are very tightly packed, we consider that the cross-sectional area of the space between adjacent axons can range from a tenth to several multiples of the cross-sectional area of the axon. Based on that, we consider R to vary between 0 and 1.

Continuous Limit Approximation

Our model is a system of N coupled nonlinear PDEs, each representing one distinct cable and accompanied by an ordinary differential equation for the corresponding slow recovery variable. However, neighboring axons in fiber pathways are often very densely packed, such as the distances separating two adjacent axons are considerably small relative to the axonal diameter (Waxman & Swadlow, 1977). For this reason, we will make the approximation that the variables v^m and i^m , while being only physically defined for the axonal space, can be abstractly represented by continuous field variables v and i . If we go back to Equation 10, we notice that the last two terms can be rewritten by using the following discrete approximation of a second partial derivative (Abramowitz & Stegun, 2012):

$$\frac{\partial^2 i^m}{\partial x^2} \approx \frac{i_{q-2}^m - 2i_q^m + i_{q+2}^m}{4\delta^2},$$

then

$$i_{q-2}^m + i_{q+2}^m \approx 4\delta^2 \frac{\partial^2 i^m}{\partial x^2} + 2i_q^m,$$

where δ is the small separation between adjacent axons. Using this latter finite difference stencil, Equation 10 is transformed to

$$\frac{\partial^2 v^m}{\partial z^2} = (r_a + r_e) i^m + \delta^2 r_e \frac{\partial^2 i^m}{\partial x^2}. \tag{14}$$

This equation relates the transmembrane voltage and current approximate field variables. The second relationship between the two is given by the balance of currents Equation 4. The approximate continuous system then takes the following form:

$$\frac{\partial^2 v}{\partial z^2} = (r_a + r_e) i + \delta^2 r_e \frac{\partial^2 i}{\partial x^2}, \quad i = c \frac{\partial v}{\partial t} + g_f(v, w) - I,$$

with $\frac{\partial w}{\partial t} = \epsilon (v + a - bw),$

where the superscripts were dropped for brevity. Next, we nondimensionalize the equations using the following rescaling:

$$\tilde{z} = \left(\sqrt{g(r_a + r_e)} \right) z, \quad \tilde{t} = \frac{g}{c} t, \quad \tilde{x} = \frac{x}{\lambda}.$$

Here, λ is a characteristic lateral length scale of the same order of magnitude as the average axonal diameter (μm). The resulting system becomes

$$\begin{aligned} \frac{\partial^2 v}{\partial \tilde{z}^2} &= i + K \frac{\partial^2 i}{\partial \tilde{x}^2}, \quad i = \frac{\partial v}{\partial \tilde{t}} + f(v, w) - \hat{I}; \\ \frac{\partial w}{\partial \tilde{t}} &= \hat{\varepsilon}(v + a - bw), \quad \text{with } K = \frac{\delta^2}{\lambda^2} \frac{1}{R + 1}. \end{aligned}$$

Dropping the tilde and hat for brevity, we obtain the final form of the approximate continuous field equations for a sheet of ephaptically coupled axons:

$$\begin{aligned} \frac{\partial^2 v}{\partial z^2} &= i + K \frac{\partial^2 i}{\partial x^2}, \quad i = \frac{\partial v}{\partial t} + f(v, w) - I; \\ \frac{\partial w}{\partial t} &= \varepsilon(v + a - bw). \end{aligned} \tag{15}$$

We note here that the latter equations governing v and i can be transformed into a more compact form of one partial integro-differential equation using Green's function and contour integration, such that the system becomes the following:

$$\begin{aligned} \frac{\partial v(x, z, t)}{\partial t} &= -F(v, w) + I + \int g(x, x') \frac{\partial^2 v(x', z, t)}{\partial z^2} dx', \\ \frac{\partial w(x, z, t)}{\partial t} &= \varepsilon(v + a - bw), \end{aligned}$$

$$\text{where } g(x, x') = g(x - x') = \frac{1}{\sqrt{K}} \sin\left(\frac{1}{\sqrt{K}}(x - x')\right).$$

In the results that follow, we take $\frac{\delta^2}{\lambda^2} \approx 0.01$, to be consistent with the assumption that the interaxonal spacing is very small compared with the characteristic length. Hence, we consider values of K in the range of 0 to 0.1 to be in line with the above choice of R being between 0 and 1.

We also note that the model can be extended to the 3D case by considering axons on a two-dimensional grid (x, y) instead of a 1D line (x) . While deriving the N coupled PDE system will be more tedious in this case, the continuous limit approximation leads to Equation 15 with one added term on the right-hand side of the first equation:

$$\begin{aligned} \frac{\partial^2 v}{\partial z^2} &= i + K \left(\frac{\partial^2 i}{\partial x^2} + \frac{\partial^2 i}{\partial y^2} \right), \quad i = \frac{\partial v}{\partial t} + f(v, w) - I; \\ \frac{\partial w}{\partial t} &= \varepsilon(v + a - bw). \end{aligned} \tag{16}$$

Numerical Implementation

Numerical solutions of the two model systems were obtained using the Crank-Nicolson finite difference method. After numerical experiments were performed with smaller values and

Green's function:
An integral transform that aids in reformulating and solving differential equations.

confidence in the stability of the solution was established, we chose a time step of 0.05 and a spatial step of 0.5 and 1 for the z and x directions, respectively. Zero flux boundary conditions were enforced, such that the first spatial derivative of v remains 0 at the boundaries for all time. To investigate the response of the system, impulses were initiated at the inlet of axons using a brief and localized input current $I = 2$ applied to the axon for $t \in [0, 2]$ and $z \in [0, 4]$. All numerical computation was implemented using Python.

RESULTS

Numerical simulations were performed to investigate the dynamics of the system as the ephaptic interaction strength was varied. In addition, we compared the dynamics of the continuous limit system (Equation 15) to that of the original discrete model (Equation 13).

Phase Interactions

In Figure 3, two adjacent axons are stimulated such that an action potential is initiated along each of them and travels from left to right. The timing of the stimulation is such that one impulse lags behind the other. The shape of the action potentials and their propagation along the z -direction can be seen in the Supporting Information (SI Figure 1). In Figure 3A, where we set $R = 0.8$ corresponding to weak ephaptic coupling, the two impulses travel independently without influencing each other. In Figure 3B and C, for the same value of R but with the stimulated axons directly adjacent to each other, ephaptic interaction causes the two impulses to attract/repel each other such that the lag between them decreases/increases, after which they remain locked together, depending on the initial time lag between them. This type of interaction has been experimentally observed in Katz and Schmitt (1940).

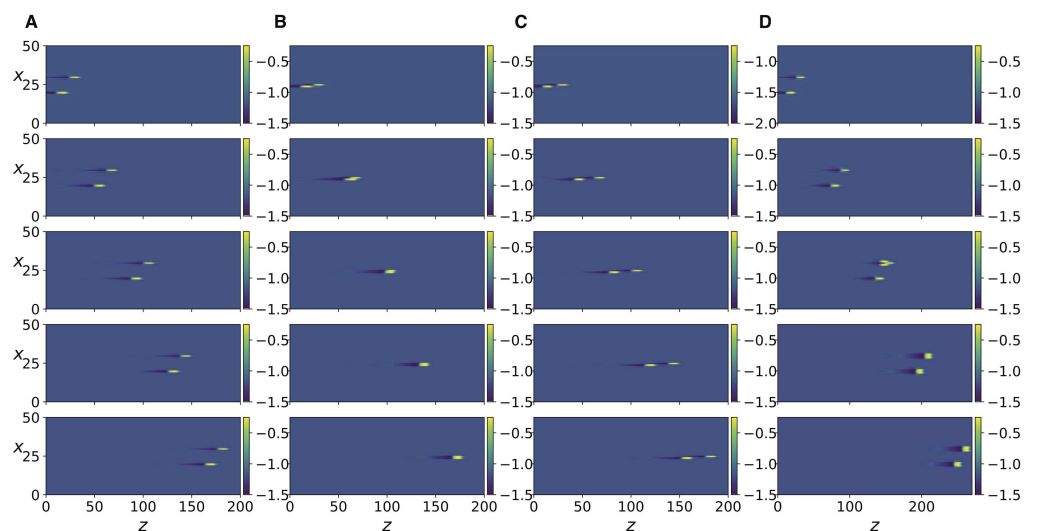


Figure 3. Numerical simulation of Equation 13. The color bar indicates the value of v , the x variable indicates the axon number. Each column corresponds to a simulation with a specific value of the parameter; snapshots show progress of time from top to bottom. (A) $R = 0.8$, axons number 30 and 20 are stimulated at $t = 0$ and $t = 10$, respectively, and the panel rows from top to bottom correspond to $t = 500, 1100, 1700, 2300, 2900$. (B) Same as in A but with axons number 25 and 24 stimulated. (C) Same as in B but with stimulation at $t = 0$ and $t = 11$. (D) same as in A but with $R = 0.4$, and panels show $t = 500, 1400, 2300, 3200, 4100$.

Spatial Patterns Generation

Next, we increase the coupling strength by decreasing R , and observe that a transition occurs where each traveling impulse triggers new action potentials in its two immediately adjacent axons and the three neighboring impulses move together as a finite size traveling front, as shown in Figure 3D. Further increase in coupling strength leads to the next two adjacent axons being activated (Figure 4A). Because of the presence of the scaling factor $\frac{\delta^2}{\lambda^2}$ in the expression for K , we do not expect Equation 15 to be equivalent to Equation 13 for the same values of R . Nonetheless, it can be seen in Supporting Information Figure 2 that the same behavior described so far also occurs in Equation 15 as the coupling strength K is increased. In addition, as coupling strength is further increased, more and more impulses are triggered as the traveling front of impulses diffuses laterally and widens (Figure 5A and B). Even further increase in

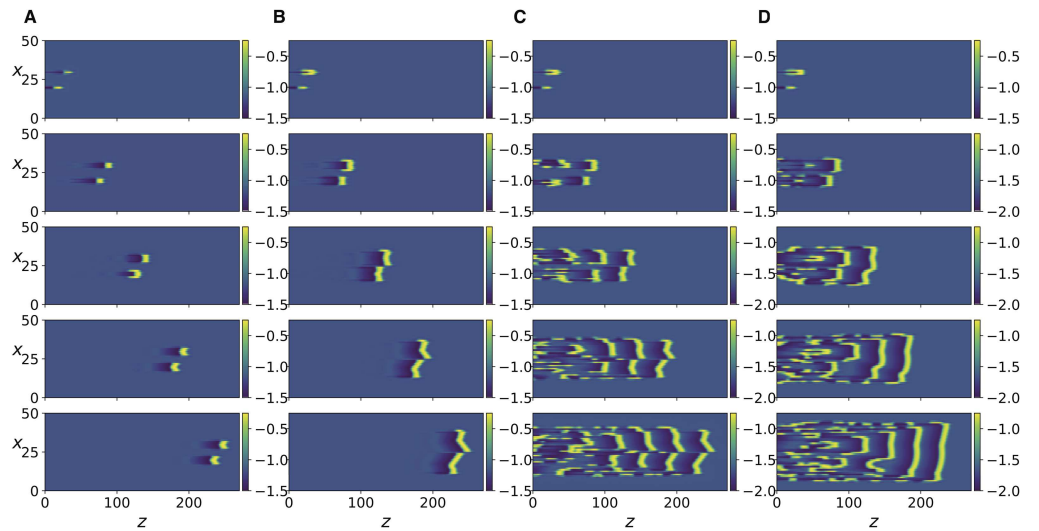


Figure 4. (A, B) same as in Figure 3A but with $R = 0.33$ and $R = 0.191$, respectively. (C, D) same as in Figure 3D but with $R = 0.19$ and $R = 0.15$, respectively.

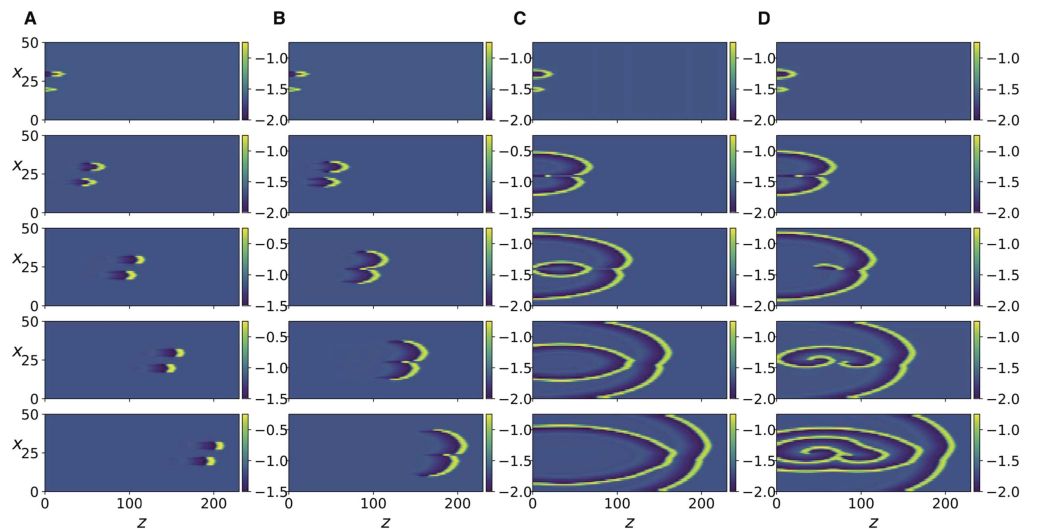


Figure 5. Same as in Figure 3 but for Equation 15, with different values of K and for $t = 500, 1300, 2200, 3100, 3999$. (A) $K = 0.0255$. (B) $K = 0.026$. (C) $K = 0.038$. (D) $K = 0.04$.

K (Figure 5C and D) leads to new fronts of impulses being induced in the forward but also backward direction, resulting in dynamic spatiotemporal patterns.

Figure 4B, C, and D show that the same transitions also occur in Equation 13 as R is decreased, albeit the resulting patterns are more discrete and irregular. To better compare the responses of the two systems in this regime, we compare the discrete Fourier transform of the spatial patterns of the two systems at several time instants (Supporting Information Figure 3). It can be seen that the spatial modal decomposition of the two is rather close, as quantified by the cosine similarity between the discrete Fourier transforms at every time step (Supporting Information Figure 4). The mean value over time was $\approx 0.96 \pm 0.006$, which indicates close similarity. However, for Equation 15, these spatiotemporal patterns persist only for a small range of the parameter, as a further increase in K causes the system to revert back to the laterally diffusing traveling front (Figure 6, right column). This is unlike Equation 13 in which the complex spatio-temporal patterns persist as R is further decreased (Figure 6, left column).

Cosine similarity:

The cosine of the angle between two vectors; computed as the dot product between the two vectors divided by the product of their magnitudes.

Poisson process:

A series of independent stochastically occurring events with a constant average time interval between events.

Spike Trains Interactions

Next, we stimulate all of the 50 axons and observe the collective dynamics. Each axon is stimulated by a finite train of 10 impulses. The intervals between impulses are generated by a Poisson process with a specified mean interval. (The mean interval is the mean value of the intervals between consecutive impulses.) The evolution of the resulting action potentials for the case of negligible ephaptic coupling is shown in Figure 7A. When ephaptic coupling becomes significant, as in Figure 7B, the impulses self-organize into phase-locked traveling fronts. A similar effect also occurs for Equation 15 (compare Figure 7C and D).

It has been stated that “in theory, whereas the pattern of Poisson-like impulse codes was modified during long-distance propagation, their mean rate was conserved” (Moradmand & Goldfinger, 1995, p. 2415). On the contrary, here in the presence of ephaptic interactions, the mean interspike interval (mISI), which is the inverse of the mean rate, decreases with increasing z location (Supporting Information Figure 5 and Supporting Information Figure 6). The effect is clearly seen when the mISI is averaged over the 50 axons at downstream z locations (Figure 8).

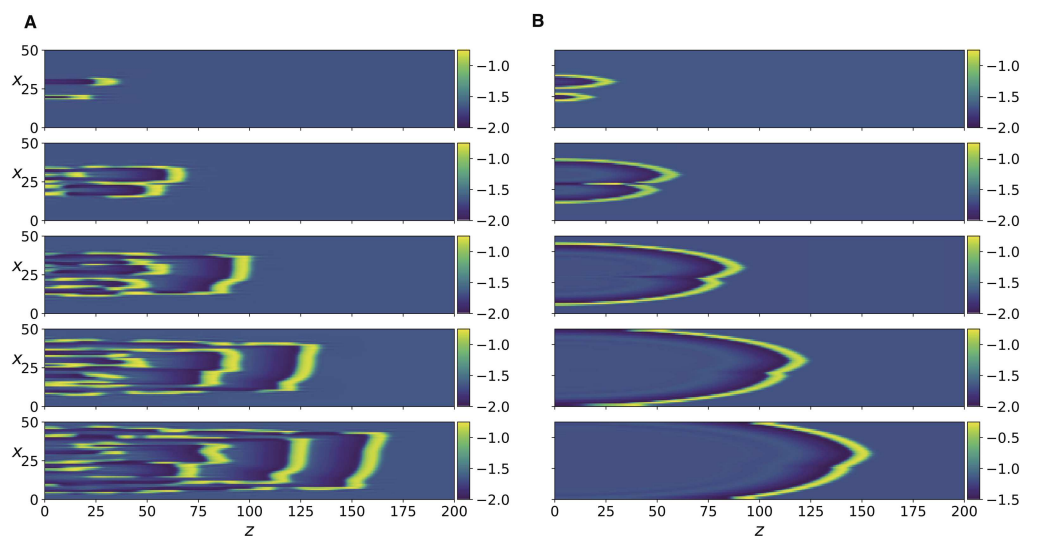


Figure 6. Numerical simulation of Equation 13 for $R = 0.05$ (left) and of Equation 15 for $K = 0.05$ (right). The panels from top to bottom correspond to $t = 500, 1100, 1700, 2300, 2900$.

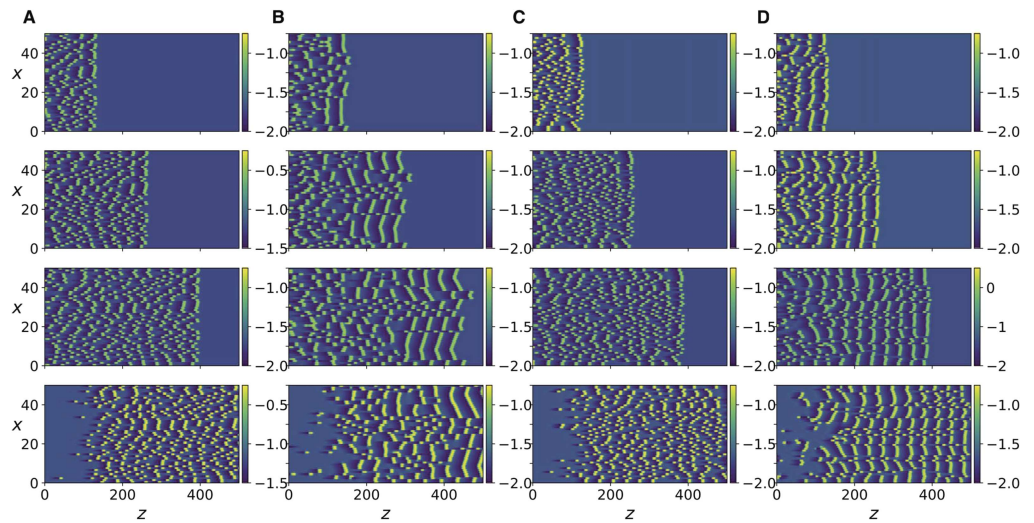


Figure 7. Numerical simulation of Equation 13 (A, B) and Equation 15 (C, D). spike trains of an average of 10 impulses are triggered along each axon, with a mean interimpulse interval of 10. The panels from top to bottom correspond to $t = 2499, 4999, 7499, 9999$.

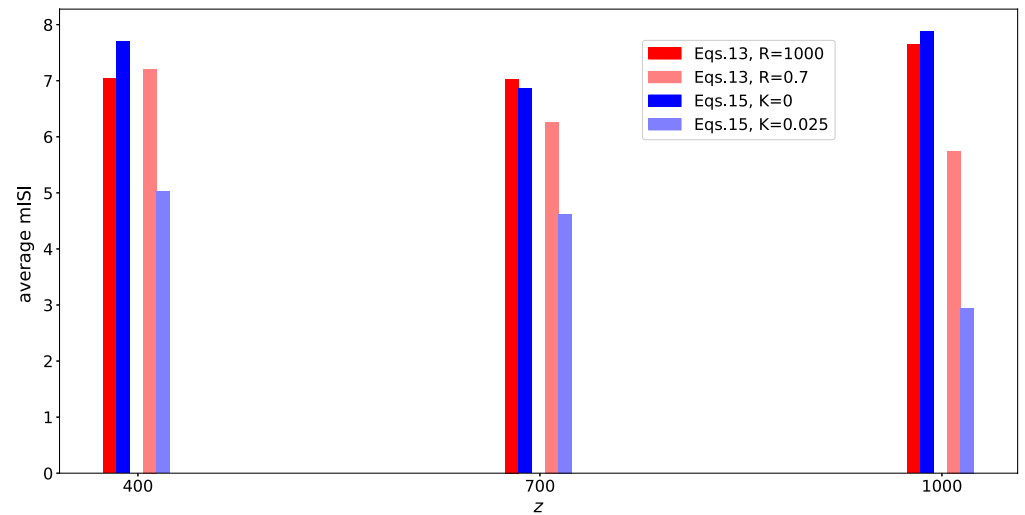


Figure 8. Mean interspike interval (mISI) averaged over the 50 axons for downstream z locations for the simulations in Figure 7A (red), 7B (light red), 7C (blue), and 7D (light blue) (low coupling in dark colors and high coupling in light colors).

Note that Figure 7 shows only a portion of the simulation; in order to compute the mISI values shown in Supporting Information Figure 5 and Supporting Information Figure 6, we let the simulation run long enough until all the impulses that were initiated at one end of the axon reach the other end, such that the total simulation time was 18,000.

DISCUSSION

We presented a minimal model for a sheet or volume of ephaptically coupled axons and explored its dynamics for a physically plausible range of parameters. We found that the model captures the experimentally observed attraction/repulsion effect between neighboring

impulses. For strong enough coupling, the model predicts that action potentials traveling down an axon can trigger new action potentials in adjacent axons to be initiated and carried along with it, forming a finite size traveling front. These fronts increase in size as more axons are recruited at higher coupling strength. Simulations with even higher coupling strength result in recurrence of impulses and backward propagation such that a pair of individual impulses initiated on two nonadjacent axons evolve into trains of impulses that diffuse laterally in the x direction as well as in both +ve and -ve z directions along the axons. We have also observed that ephaptic coupling can lead to self-organization among trains of impulses and significant alteration in the timing of action potentials, which is known to be a key element in neuronal coding (Debanne, 2004). This suggests that ephaptic interactions along fiber pathways can theoretically play an active role in neuronal signal processing in the brain. The numerical simulations showed that the continuous limit approximation system mimics the qualitative behavior of the original model for a specific range of parameters. This continuous limit model offers the advantage of being mathematically more compact, more analytically tractable, and less numerically expensive to solve, and it allows for easy extension of the model to full 3D geometry. It furthermore allows for a more intuitive interpretation of the ephaptic coupling terms and, in its integro-differential form, makes it intuitive that the ephaptic coupling creates a modulation of the diffusion in the axial direction with an alternating positive and negative diffusion term on a spatial length scale favoring structures on the scale of \sqrt{K} .

In conclusion, we propose that the various nontrivial responses observed in our numerical exploration of ephaptic interaction might play an important and complex active role in interarea neuronal signal transmission and processing in the brain. We hope these results will motivate a critical examination of the validity of the common assumption that neuronal fiber pathways merely act as transmission cables relaying signals between different brain regions. In contrast to that latter viewpoint, this theoretical investigation suggests that ephaptic interactions enhanced by the orientations and bundling of neuronal tracts in three-dimensional space can render the fiber pathways an active axonal medium that can give rise to complex spatiotemporal dynamics. If this emergent dynamics occurs under physiologically realistic conditions, then it would be a major so far unknown contributor to information processing in neural systems. We see various directions that this work can take in the future, including further exploration of the rich repertoire of responses for different types of stimuli, accounting for variability in axonal diameters that will add spatial heterogeneity in the parameters. In addition, a natural extension to a more biophysically detailed treatment of the matter is possible through incorporating the effect of myelination into the cable equation used in the model. Finally, we hope that our work will inspire experimental work that can provide precise quantification and characterization of the elusive effects of ephaptic interactions in the axonal tracts of the brain.

SUPPORTING INFORMATION

Supporting information for this article is available at https://doi.org/10.1162/netn_a_00134.

AUTHOR CONTRIBUTIONS

Hiba Sheheitli: Conceptualization; Data curation; Formal analysis; Investigation; Methodology; Validation; Visualization; Writing - Original Draft; Writing - Review & Editing. Viktor K. Jirsa: Conceptualization; Formal analysis; Funding acquisition; Investigation; Methodology; Project administration; Resources; Supervision; Writing - Review & Editing.

FUNDING INFORMATION

Viktor K. Jirsa, European Commission (<http://dx.doi.org/10.13039/501100000780>), Award ID: H2020-720270.

REFERENCES

- Abramowitz, M., & Stegun, I. (2012). *Handbook of mathematical functions: With formulas, graphs, and mathematical tables*. New York, NY: Dover Publications.
- Anastassiou, C. A., & Koch, C. (2015). Ephaptic coupling to endogenous electric field activity: Why bother? *Current Opinion in Neurobiology*, *31*, 95–103.
- Anastassiou, C. A., Perin, R., Markram, H., & Koch, C. (2011). Ephaptic coupling of cortical neurons. *Nature Neuroscience*, *14*, 217–223.
- Arvanitaki, A. (1942). Effects evoked in an axon by the activity of a contiguous one. *Journal of Neurophysiology*, *5*(2), 89–108.
- Barr, R. C., & Plonsey, R. (1992). Electrophysiological interaction through the interstitial space between adjacent unmyelinated parallel fibers. *Biophysical Journal*, *61*(5), 1164–1175.
- Bassett, D. S., Zurn, P., & Gold, J. I. (2018). On the nature and use of models in network neuroscience. *Nature Reviews Neuroscience*, *19*, 566–578.
- Bell, J. (1981). Modeling parallel, unmyelinated axons: Pulse trapping and ephaptic transmission. *SIAM Journal on Applied Mathematics*, *41*(1), 168–180.
- Binczak, S., Eilbeck, J. C., & Scott, A. C. (2001). Ephaptic coupling of myelinated nerve fibers. *Physica D: Nonlinear Phenomena*, *148*(1–2), 159–174.
- Blot, A., & Barbour, B. (2014). Ultra-rapid axon-axon ephaptic inhibition of cerebellar Purkinje cells by the pinceau. *Nature Neuroscience*, *17*, 289–295.
- Bokil, H., Laaris, N., Blinder, K., Ennis, M., & Keller, A. (2001). Ephaptic interactions in the mammalian olfactory system. *Journal of Neuroscience*, *21*(20), RC173.
- Breakspear, M. (2017). Dynamic models of large-scale brain activity. *Nature Neuroscience*, *20*, 340–352.
- Clark, J., & Plonsey, R. (1968). The extracellular potential field of the single active nerve fiber in a volume conductor. *Biophysical Journal*, *8*(7), 842–864.
- Clark, J. W., & Plonsey, R. (1970). A mathematical study of nerve fiber interaction. *Biophysical Journal*, *10*(10), 937–957.
- Debanne, D. (2004). Information processing in the axon. *Nature Reviews Neuroscience*, *5*, 304–316.
- FitzHugh, R. (1961). Impulses and physiological states in theoretical models of nerve membrane. *Biophysical Journal*, *1*(6), 445–466.
- Fröhlich, F., & McCormick, D. A. (2010). Endogenous electric fields may guide neocortical network activity. *Neuron*, *67*(1), 129–143.
- Goldwyn, J. H., & Rinzel, J. (2016). Neuronal coupling by endogenous electric fields: Cable theory and applications to coincidence detector neurons in the auditory brain stem. *Journal of Neurophysiology*, *115*(4), 2033–2051.
- Grindrod, P., & Sleeman, B. D. (1984). Qualitative analysis of reaction-diffusion systems modelling coupled unmyelinated nerve axons. *Mathematical Medicine and Biology*, *1*(3), 289–307.
- He, B., Yang, L., Wilke, C., & Yuan, H. (2011). Electrophysiological imaging of brain activity and connectivity—Challenges and opportunities. *IEEE Transaction on Biomedical Engineering*, *58*(7), 1918–1931.
- Hodgkin, A. L., & Huxley, A. F. (1952). A quantitative description of membrane current and its application to conduction and excitation in nerve. *Journal of Physiology*, *117*(4), 500–544.
- Holt, G. R., & Koch, C. (1999). Electrical interactions via the extracellular potential near cell bodies. *Journal of Computational Neuroscience*, *6*(2), 169–184.
- Katz, B., & Schmitt, O. H. (1940). Electric interaction between two adjacent nerve fibres. *Journal of Physiology*, *97*(4), 471–488.
- Lamantia, A. S., & Rakic, P. (1990). Cytological and quantitative characteristics of four cerebral commissures in the rhesus monkey. *Journal of Comparative Neurology*, *291*(4), 520–537.
- Marrazzi, A. S., & Lorente, R. (1944). Interaction of neighboring fibres in myelinated nerve. *Journal of Neurophysiology*, *7*(2), 83–101.
- Moradmand, K., & Goldfinger, M. (1995). Computation of long distance propagation of impulses elicited by Poisson-process stimulation. *Journal Neurophysiology*, *74*(6), 2415–2426.
- Nagumo, J., Arimoto, S., & Yoshizawa, S. (1962). An active pulse transmission line simulating nerve axon. *Proceedings of the IRE*, *50*(10), 2061–2070.
- Nielsen, V. K. (1984). Pathophysiology of hemifacial spasm: I. Ephaptic transmission and ectopic excitation. *Neurology*, *34*(4), 418–426.
- Plonsey, R. (1977). Action potential sources and their volume conductor fields. *Proceedings of the IEEE*, *65*(5), 601–611.
- Rall, W. (1962). Electrophysiology of a dendritic neuron model. *Biophysical Journal*, *2*(2), 145–167.
- Ramón, F., & Moore, J. W. (1978). Ephaptic transmission in squid giant axons. *American Journal Physiology*, *234*(5), C162–C169.
- Rasminsky, M. (1980). Ephaptic transmission between single nerve fibres in the spinal roots of dystrophic mice. *Journal of Physiology*, *350*, 151–169.
- Reutskiy, S., Rossoni, E., & Tirozzi, B. (2003). Conduction in bundles of demyelinated nerve fibers: Computer simulation. *Biological Cybernetics*, *89*(6), 439–448.
- Rosenblueth, A. (1941). The stimulation of myelinated axons by nerve impulses in adjacent myelinated axons. *American Journal of Physiology*, *132*(1), 119–128.
- Sanz-Leon, P., Knock, S. A., Spiegler, A., & Jirsa, V. K. (2015). Mathematical framework for large-scale brain network modeling in The Virtual Brain. *NeuroImage*, *111*, 385–430.
- Scott, A. (2002). *Neuroscience: A mathematical primer*. New York, NY: Springer US.
- Stacey, R. G., Hilbert, L., & Quail, T. (2015). Computational study of synchrony in fields and microclusters of ephaptically coupled neurons. *Journal of Neurophysiology*, *113*(9), 3229–3241.

Taylor, C., & Dudek, F. (1982). Synchronous neural afterdischarges in rat hippocampal slices without active chemical synapses. *Science*, 218(4574), 810–812.

Usmani, R. A. (1987). *Applied linear algebra*. New York, NY: Marcel Dekker.

Waxman, S. G., & Swadlow, H. A. (1977). The conduction properties of axons in central white matter. *Progress in Neurobiology*, 8, 297–324.

Wedeen, V. J., Rosene, D. L., Wang, R., Dai, G., Mortazavi, F., Hagmann, P., . . . Tseng, W. Y. I. (2012). The geometric structure of the brain fiber pathways. *Science*, 335(6076), 1628–1634.